NUMERICAL MODELING OF ROCK RIDGE BREAKAGE IN ROTARY CUTTING

B. Yu
Agapito Associates, Inc., Grand Junction, Colorado, USA

A. W. Khair
West Virginia University, Morgantown, West Virginia, USA

ABSTRACT: In this paper, the finite element code LS-DYNA 3D was chosen as the simulation tool to study the rotary rock cutting process. By using an Automated Rotary Rock Cutting Simulator as the prototype, a numerical model of a continuous miner was developed. The rock grooves cut by the bits in the numerical model were used to investigate the rock ridge failure mechanism. The numerical study indicated that shear breakage acted as the dominant mechanism in ridge removal. Drum speed, depth of cut and multiple bit interaction have minimal effects on the groove width. For a given bit pattern, Young's modulus and Poisson ratio of the rock are two major parameters affecting the ridge removal.

1 INTRODUCTION

Rotary cutting machines, such as continuous miners and shears are widely utilized in underground soft rock mining (e.g. coal mining and salt mining). These machines usually use cylinder-shaped cutting drums on which bits are laced based on certain patterns. During work, the rotating drum sumps into the rock face with bits cutting the rock. Breakage of the rock ridges between the bits occurs when the bits hit the rock. Two contradictory theories exist to explain the mechanism of rock ridge breakage. One of the fundamental rock cutting theories was proposed by Evans (Evans, et al, 1966), who considered the rock ridge breakage as tensile rock failure. This theory was utilized by other researchers to explain the general failure phenomenon of rocks (Whittaker, et al 1973, Roxborough, 1973). While on the other hand, Nishimatsu (1972) assumed shear strength of the rock is the dominant parameter governing rock failure.

The intention of this paper is to evaluate the theories on rock ridge breakage mechanism during rotary rock cutting based on numerical experiments. The numerical model used to simulate rotary rock cutting is first described in section 2. Some numerical experiments are then conducted and the results are analyzed in section 3. Conclusions drawn from the analysis are listed in the last section.

2 NUMERICAL SIMULATION OF ROTARY ROCK CUTTING

An Automated Rotary Rock Cutting Simulator (ARCCS) shown in Figure 2.1 was chosen as the prototype for the numerical model. This simulator has been used to conduct rock cutting experiments for twenty years at West Virginia University and vast experimental data can be used directly to calibrate the numerical model. LS-DYNA 3D was chosen as the simulation tool because of its ability to simulate dynamic processes. Figure 2.2 shows the cutting drum of the ARCCS and a piece of rock discretized in elements. The rock element size was about 7.6mm × 7.6mm × 7.6mm. Quiet boundaries were applied on lateral and back boundaries of the rock in order to absorb body waves created by bit impact approaching the boundaries in both normal and shear directions. By using this boundary scheme, an infinite rock medium was simulated before the cutting drum. In order to further relieve the computational burden, rigid material properties were assigned to the bits, bit holders and drum body. The average bit spacing was 45.7mm. The detail model setup and calibration has been published in other paper (Yu & Khair, 2005).

Figure 2. 1 The automatic rock & coal rotary cutting simulator

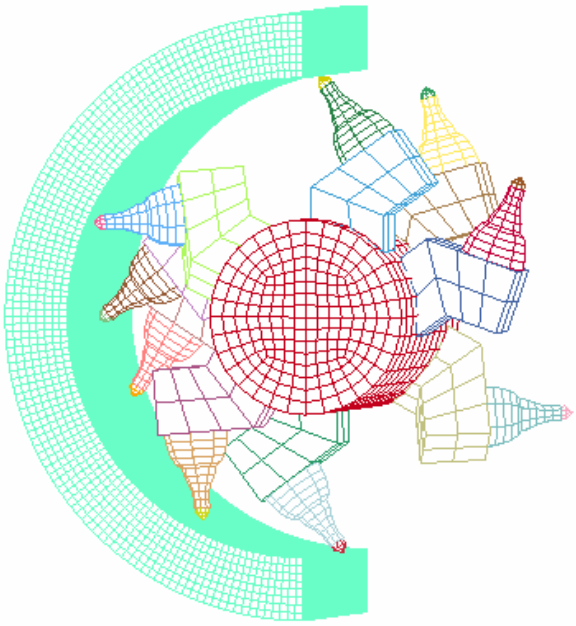

Figure 2. 2 Cutting drum and rock in elements

In rotary rock cutting, bit-rock interaction consists of the basic mechanism of rock fragmentation. Interaction algorithm with erosion (Belytschko & Lin, 1984) was utilized to simulate the fragmentation process by eroding failed rock elements. This algorithm uses a concept of slave nodes and master elements. One of the two interaction bodies, usually a bit, is defined by the slave nodes; the second body, the rock, is defined by the master elements. The mechanics of the interaction of the two bodies is executed completely through the interaction of the slave nodes with the master elements. The rules of this interaction are summarized as follows:

(1) Slave nodes are not permitted to penetrate master elements.
(2) Whenever penetration of a slave node into a master element is detected, the slave node is returned to the surface of the element it has penetrated and the associated loss of momentum is transferred to the appropriate nodes of the master element.

Two failure criteria were used for the rock material. One was the tensile failure criterion expressed in Equation 2.1, and the other is the shear failure criterion expressed in Equation 2.2.

$$\sigma_1 \geq \sigma_t \qquad (2.1)$$

where σ_1 is the maximum principal stress,

σ_t is the tensile strength of the rock.

$$\sqrt{\frac{3}{2}\sigma'_{ij}\sigma'_{ij}} \geq \sigma_c \qquad (2.2)$$

where σ_c is the simple compressive strength of the rock.

σ'_{ij} are the deviatoric stress components, and

$$\sigma'_{ij} = \sigma_{ij} - p\delta_{ij} \qquad (2.3)$$

$$p = \frac{1}{3}\sigma_{kk} = \frac{1}{3}I_1 \qquad (2.4)$$

where σ_{ij} is Cauchy stresses,

I_1 is sum of the diagonal terms of σ_{ij}.

Figure 2.3 and Figure 2.4 are the plots of the cutting process captured at different time points during the computation. The bright points are the nodes belonging to the deleted elements. The deleted elements in the rock represent the excavated material. The cutting grooves in the computer model and the grooves cut in a lab cutting experiment under similar cutting conditions are presented in Figure 2.5 for comparison. Both the simulation and the experiments showed that in a rotary cutting action the shape of the groove cut by an individual bit resembles a crescent. Each bit on the drum starts the cutting face from zero depth of cut and as the bits penetrate further into the rock face, the depth of cut increases to a maximum at the vertical center line of the path of each cutting bit, then the depth of cut decreases to zero when the bit exits the cutting face.

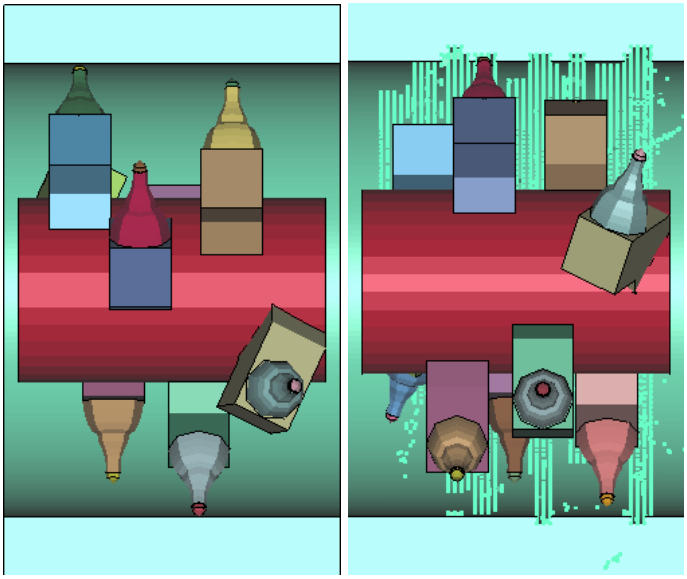

(a) 0 revolution
0 cut depth

(b) 1.17 revolutions
3.6mm cut depth

(c) 2.34 revolutions
7.1mm cut depth

(d) 3.51 revolutions
10.6mm cut depth

(e) 4.68 revolutions
14.2mm cut depth

(f) 5.85 revolutions
17.8mm cut depth

Figure 2. 3 Various time stages in the cutting process

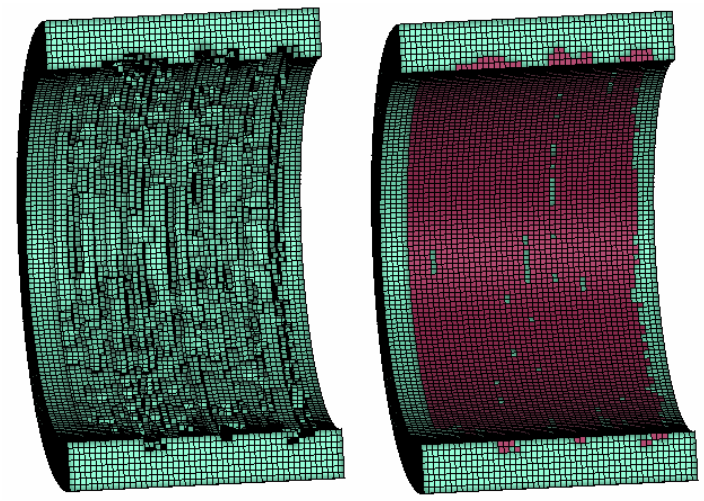

(a) Grooves cut in the model

(b) Deleted elements highlighted

(c) Rock grooves cut in lab test

Figure 2. 1 Cutting grooves comparison

3. NUMERICAL EXPERIMENTS AND ANALYSIS

Before the rotary cutting model was utilized in numerical studies, it has been calibrated by the experiment data, i.e. the rock properties were adjusted so that the average thrust and cutting force applied by the drum in the numerical model were at the same force magnitudes applied in the lab test, assuming under the similar cutting conditions. In the study of rock failure mode during rotary cutting, several numerical tests were conducted for single bit cutting. In the first test, both shear and tensile failure criteria were used for the rock material. In the second run, only tensile failure was allowed during rock cutting. And in the third run, only shear failure was applied.

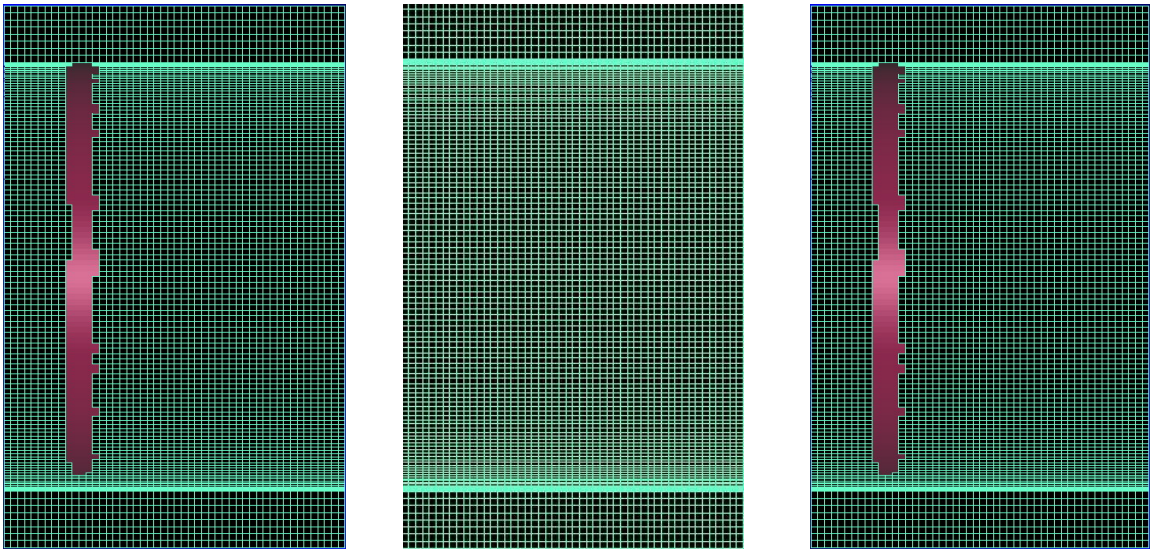

Figure 3. 1 Cutting grooves of bit 1 in three numerical tests

(left: both shear and tensile failure criteria were used; middle: only tensile failure was allowed; right: only shear failure was used.)

The grooves obtained from these three tests are highlighted in Figure 3.1. The result indicated that no tensile failure occurred during cutting intact rock, which is apparently opposed to Evan's theory. In order to check the erosion algorithm's ability of simulating tensile failure, a model of a projectile penetrating a rock plate was built. This plate was only 6.35mm in thickness, so tensile stress must be generated in it due to the strike of the projectile. Figure 3.2 shows the half model of both the projectile and the rock plate.

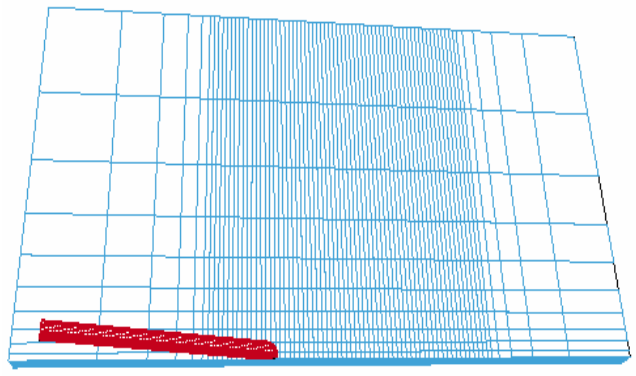

Figure 3. 2 A projectile penetrates a rock plate

In this model, only tensile failure mode was allowed for the rock plate. After the projectile penetrated through the plate, a large number of tensile failure elements were found in the rock. Figure 3.3 shows the penetration results, in which an irregular hole was torn on the rock plate by the projectile. Through this test, the algorithm's ability to simulate tensile failure in rock was verified.

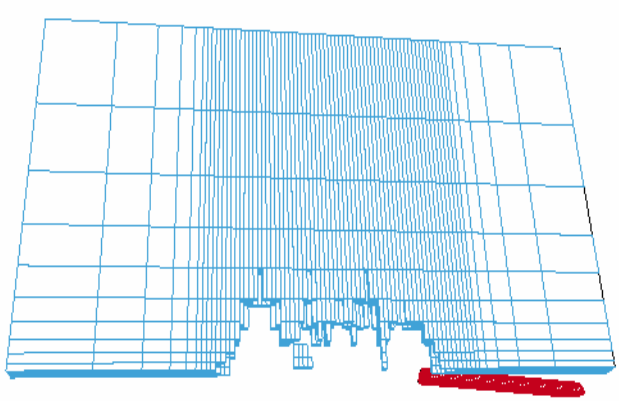

Figure 3. 3 The projectile penetrated through the rock plate

The above studies clearly showed that shear failure causes the rock breakage during rotary cutting an unbounded homogeneous rock medium. Then, the next question is how the shear stress affects the rock ridge removal, i.e. what the mechanism of rock ridge removal is. Figure 3.4 illustrates the interaction of a bit and a rock element, and rock nodal force directions due to bit impact. All nodal forces are pointing out and downward from the element. If there are adjacent elements around this element, then it will squeeze its adjacent elements when the bit penetrates into this element. These lateral forces are the ones that remove the ridge. Therefore, the larger these forces are, the larger the area of the ridge will be removed. And the steeper they are, the deeper the ridge will be removed.

In reality, it was observed that the rock underneath the bit is first crushed and then recompacted in a very short time to gain a very high stiffness and sticks to the bit (Nishimatsu, 1972, Evans, 1966). The energy release of this high stiffness element can generate huge lateral forces. In order to simulate this phenomenon, a very high stiffness can be assigned

to the rock material so that before a rock element is crushed and deleted from the model, it can accumulate very high internal energy. Another approach to increase the lateral forces should be to increase the Poisson's ratio of the rock material. Based on this analysis, it is predicted that increasing the Young's modulus and Poisson's ratio together would greatly increase the removed ridge volume.

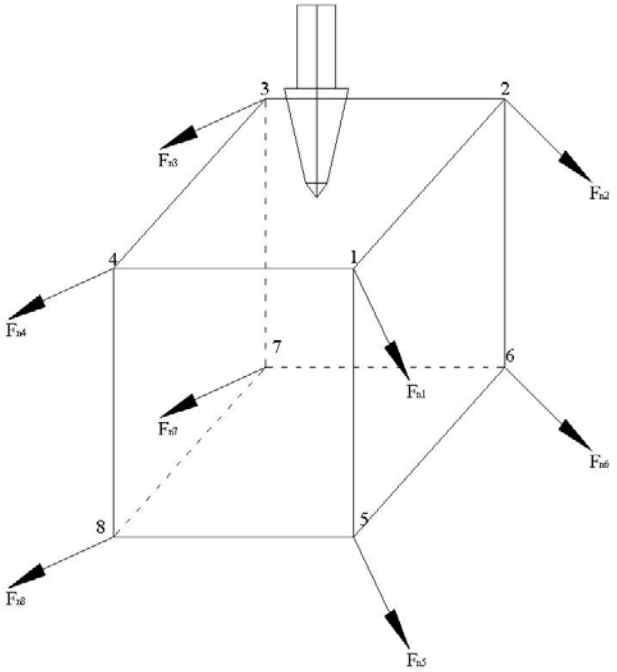

Figure 3. 4 Nodal forces in a rock element due to bit penetration

To prove this conjecture, a series of numerical tests were carried out on the cutting model (shown in Figure 3.5). In the first model, two adjacent bits on the drum were used to cut a rock medium with a Young's modulus of the rock of 2GPa and a Poisson's ratio of 0.33. In the second model a larger Young's modulus, 20GPa, was used for the rock material. And in the third model, the Young's modulus of the rock material was 20GPa and its Poisson's ratio was increased to 0.49. As shown in Figure 3.5, the ridge between the grooves was greatly reduced after the two parameters were both increased.

In order to further study the effects of the Young's modulus and the Poisson's ratio on the cutting result, a numerical model shown in Figure 3.6 was built so that the drum can be fed into the rock 38.1mm and then cut down 241.3mm. In this model, the Young's modulus of the rock was 20GPa and its Poisson's ratio was 0.49. During rock cutting simulation, only the bit tips were allowed to cut the rock. Figure 3.6 shows the cutting model and the cutting result. It clearly shows that all the ridges were removed and a clear face was left.

Other numerical tests were run to analyze the effects of multiple bit interaction, cutting depth, drum speed, and rock compressive strength on the ridge removal. Shown in Figure 3.7 the grooves were identical in single bit cutting and two adjacent bit cutting. Two adjacent bit tip cutting shown in Figure 3.8 was studied as the cutting depth from 0 to 38.1mm. It was noted that the groove width kept unchanged after cutting depth reached 25.4mm, which implied that if the bit body were not allowed to impact the rock, the groove would not become wider as the bit tip cutting deeper into the rock. The drum advance rate can not change the width of the groove either. Shown in Figure 3.9, as the drum advance rate increased from 5m/sec to 10m/sec, the groove width did not become wider.

The rock compressive strength has only a minor effect on ridge removal, since when the compressive strength of the rock underneath the bit is increased in order to accumulate more energy, whole rock strength is increased and the rock around the bit becomes more difficult to cut. Shown in Figure 3.10, the grooves of two bit tip cutting became a little bit wider as the rock compressive strength increased from 3.4MPa to 10.3MPa.

3 CONCLUSIONS

Both Evan's and Nishimatsu's theories of rock breakage during rock cutting were based on experimental results. Because of the inhomogeneity of the rock material and the difficulties encountered with specimen preparation, experiments of the same kind rock may yield widely scattered results and totally different theoretical explanations. In this numerical study, the rock breakage theory was examined on homogeneous rock materials. And it was found that for an intact homogeneous rock:

- Shear breakage acts the dominant mechanism in rotary rock cutting.
- Young's modulus and Poisson ratio are two important parameters which affect the ridge removal. For designing a drum to cut brittle materials, the bit spacing can be larger. And if the Poisson's ratio of the rock is large, the bit spacing can be widened further.
- Drum speed, depth of cut, and multiple bit interaction do not affect the groove width during cutting. Rock compressive strength only has limited influence on groove width.

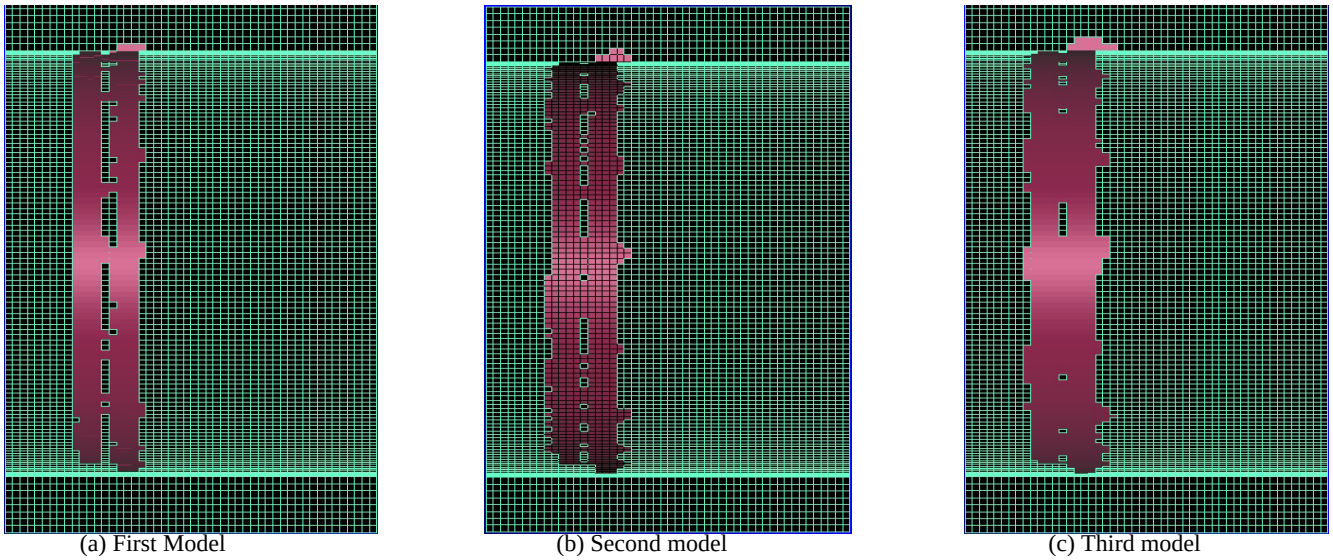

(a) First Model (b) Second model (c) Third model

Figure 3. 5 E and μ effect on the ridge removal

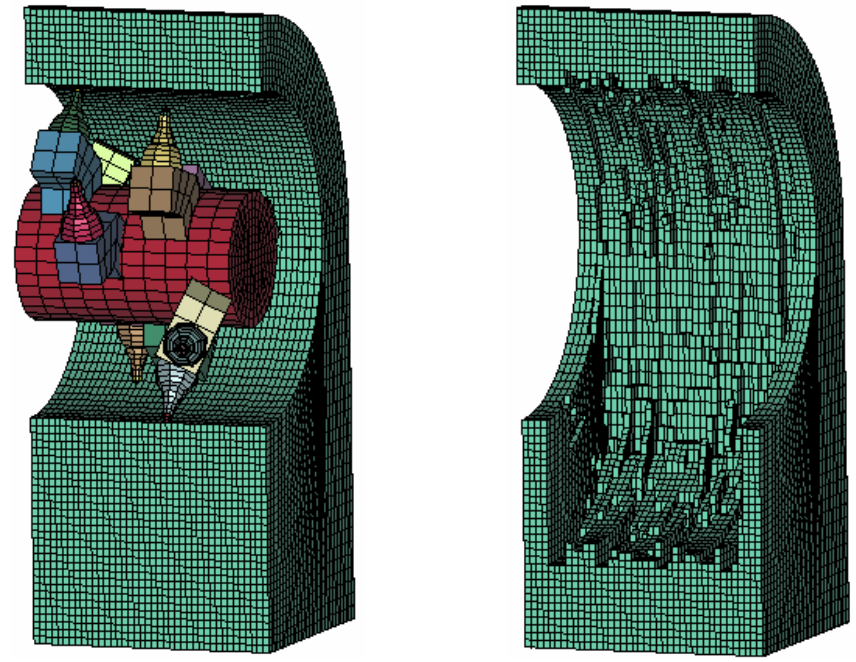

(a) Initial set up of the model (b) Cutting face after 38.1mm sumping and 241.3mm cutting

Figure 3. 6 Sumping and cutting action in high E and μ value rock cutting

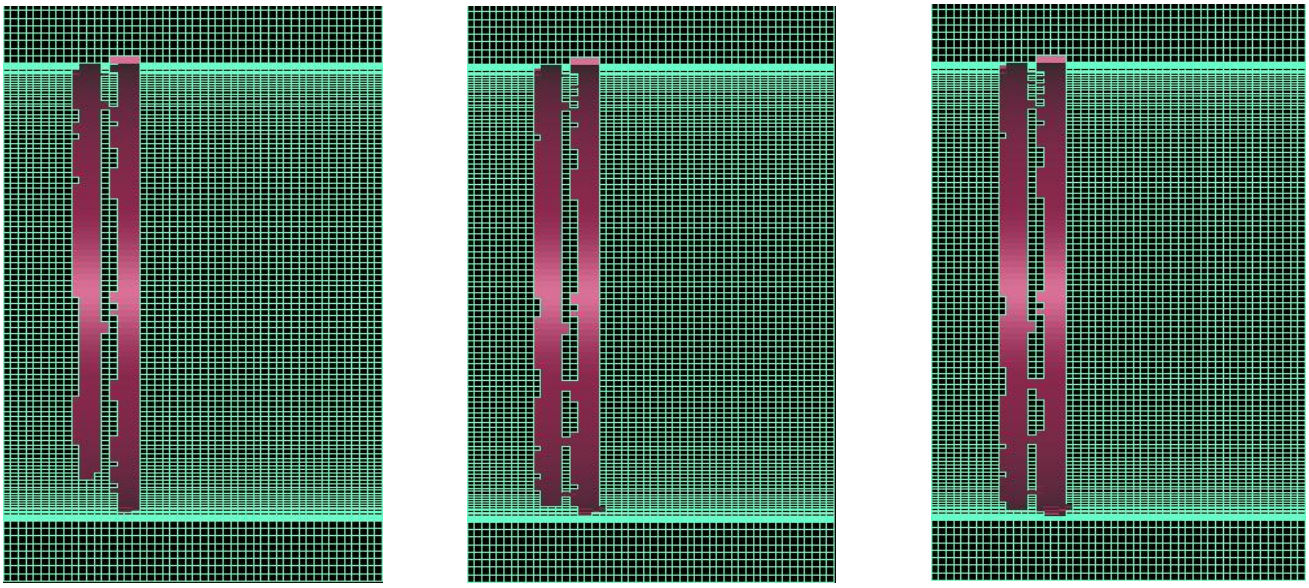

(a) Single bit cutting (b) Double bit cutting (c) Single bit cutting

Figure 3. 7 Two bit interaction test

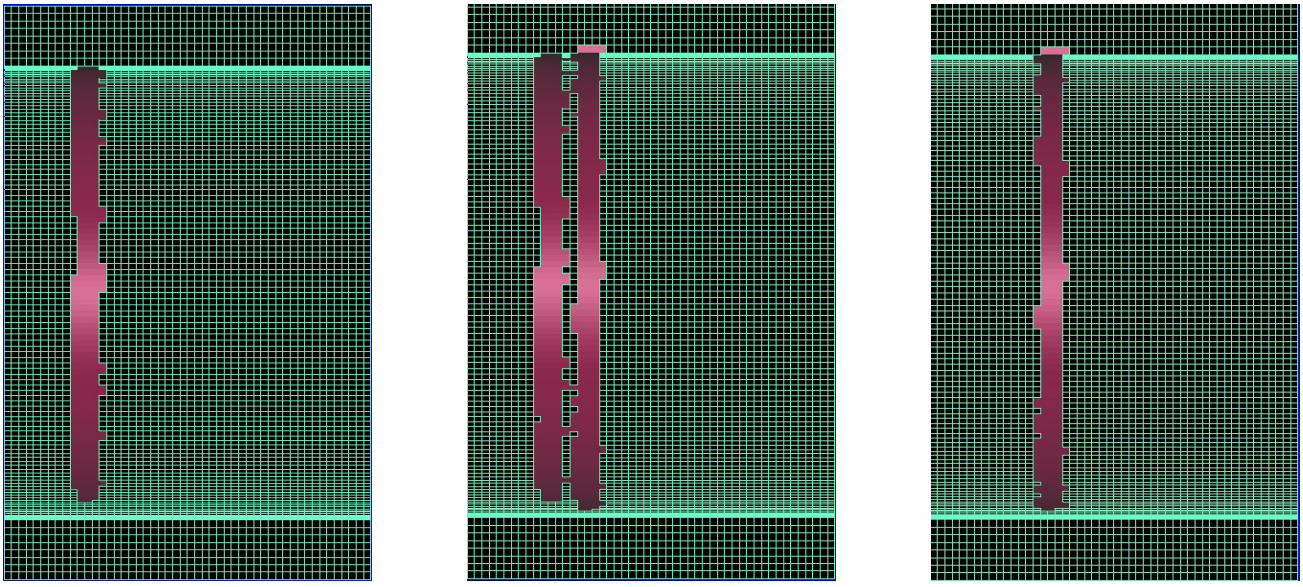

(a) Cutting depth = 12.7mm (b) Cutting depth = 25.4mm (c) Cutting depth = 38.1mm

Figure 3. 8 Cutting depth effect on the ridge removal

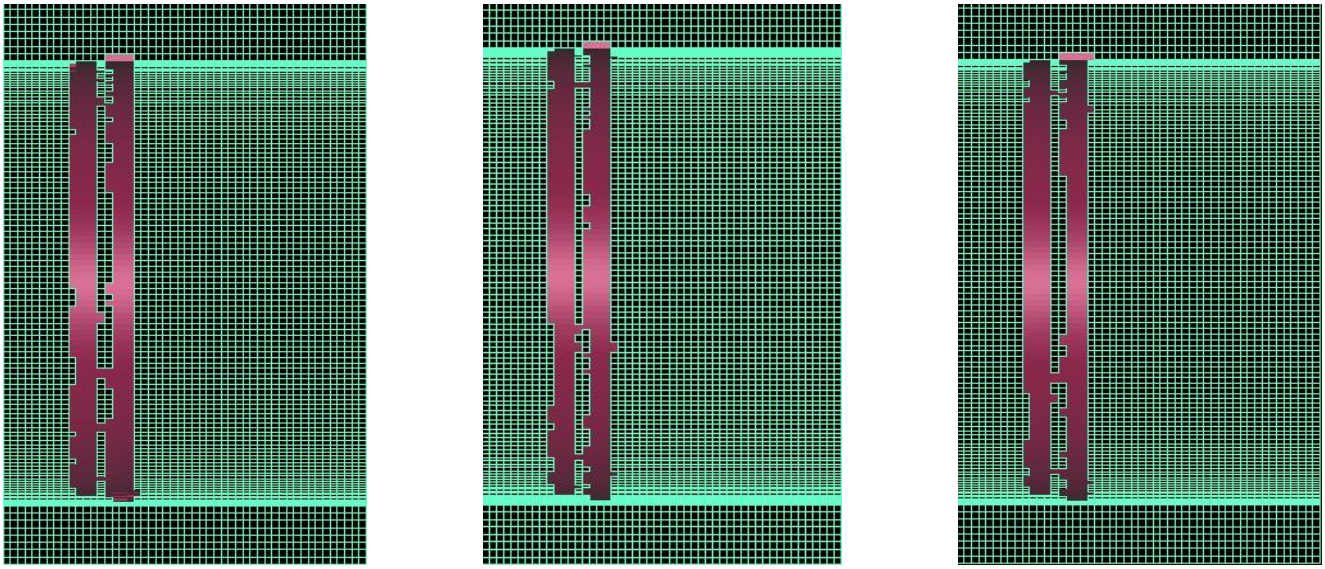

(a) Advance rate = 5m/sec (b) Advance rate = 7.5m/sec (c) Advance rate = 10m/sec

Figure 3. 9 Drum advance rate effect on the ridge removal

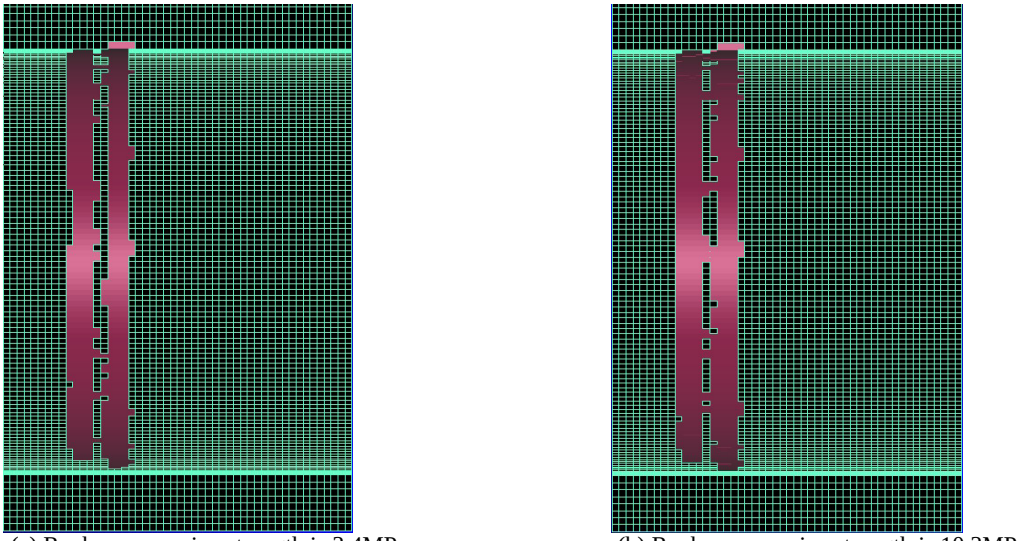

(a) Rock compressive strength is 3.4MPa (b) Rock compressive strength is 10.3MPa

Figure 3. 10 The rock compressive strength effect on ridge removal

REFERENCES

Belytschko, T. & Lin, J. I. 1987. A three dimensional impact penetration algorithm with erosion, Computers and Structures Vol. 25, No. 1 pp95-104.

Evans, I. & Pomeroy, C.D. 1966. Strength, fracture, and workability of coal. Pergamon, New York, 277pp.

Nishimatsu, Y. 1972. The mechanics of rock cutting. International Journal of Rock Mechanics and Mining Sciences Vol. 9 pp261-270.

Roxborough, F. F. 1973. Cutting rocks with picks. Mining Engineer, Vol. 132, No. 153, pp.445-454.

Whittaker, B. N. & Szwilski, A. B. 1973. Rock cutting by impact action. Int. J. Rock Mech. Min. Sci. Geomech Abstr., vol.9, pp.659-671.

Yu, B. & Khair, A.W. 2005. Computer Generated Evaluation of Cutting Drum for Continuous Miner. Proc. 4th International Conference Mining Techniques. Krakow – Krynica, Poland.